CrossMark

Adsorption properties of *Pseudomonas monteilii* for removal of uranium from aqueous solution

Xiangyi Deng[1] · Yali Feng[1] · Haoran Li[2] · Fei Yuan[1] · Qing Teng[1] · Hongjun Wang[1]

Abstract

The *Pseudomonas monteilii*. YL-1 was cultured from deep sea sediment to remove uranium from aqueous solution. Different influence factors on uranium adsorption efficiency were investigated. The kinetic model of *Pseudomonas monteilii* could be described by the pseudo-second-order kinetic model, and the Freundlich isotherm model could fit the experiment data well, indicating that the adsorption was multilayer adsorption. The adsorption was spontaneous and endothermic reaction by thermodynamic analysis. The functional groups of *Pseudomonas monteilii* such as hydroxy, carboxyl, amino and amide may act with UO_2^{2+} by chemisorption or strong complexation in the process of uranium adsorption.

Keywords *Pseudomonas monteilii* · Uranium adsorption · Kinetics · Thermodynamics

Introduction

With the development of the global nuclear energy industry and the treatment of decommissioned nuclear facilities, the harm of low radionuclides to human–environment is becoming more and more serious [1]. The uranyl ion is the main form of uranium in aqueous and has great potential to generate complex organic ligands with high solubility [2, 3]. These substances can easily be brought into human ecosystem, and the radioactive and chemical toxicity of uranyl ions can cause irreversible damage to human due to easy diffusion solubility [4]. So it is urgent to remove of uranium (VI) from aqueous system. Several methodologies of uranium removal processes have been developed, such as chemical precipitation [5], ultrafiltration [6], extraction [7], membrane separation [8] and so on. Compared with those conventional methods, the adsorption has some advantages of low operation cost, short operation time, high efficiency at low metal concentration, selectivity of uranium adsorption, and no secondary pollution [9]. Many adsorbents can be used for the removal of uranium, including inorganic adsorbents such as kaolin, illitic soil, imvite, zeolite et al. and organic adsorbents such as ion exchange resin. The main adsorption mechanism of those materials is ion exchange [10]. The other ions existed in aqueous solution have significant interference on the uranium adsorption and the capacity of those adsorbents is also limited by ion exchange process. As an economical and efficient method, bio-adsorption is considered to be an effective and promising treatment for the removal of uranium in aqueous solution. The bio-adsorbents used for uranium separation mainly include bacteria, fungi, and algae [11–13]. Sar Pinaki [14] and Kapoora Anoop [15] reported that the uranium adsorption amount can be reached at 541 mg/g and 215 mg/g by using pseudomonas aeruginosa and aspergillus niger, respectively. However, the microorganisms used as uranium adsorbents are mainly come from the land, rare researches about marine microorganisms are reported [16, 17].

Because of the particularity of the marine environment (high salt, high pressure, low temperature, less light and so on) and the function of microorganisms in the ecosystem,

✉ Yali Feng
  ylfeng126@126.com

✉ Haoran Li
  hrli@ipe.ac.cn

1   School of Civil and Resource Engineering, University of Science and Technology Beijing, Beijing 100083, China

2   State Key Laboratory of Biochemical Engineering, Institute of Process Engineering, Chinese Academy of Science, Beijing 100090, China

marine microorganisms have their own special species and unique metabolic methods, which make marine-derived adsorbents more beneficial to removal heavy metal ions [18]. The rich functional groups on the surface of marine-derived adsorbents can act with uranyl ions by complexation. In this work, the *Pseudomonas monteilii*. YL-1 was obtained from deep sea sediment to remove uranium from aqueous solution. The adsorption behavior has been studied in a batch reactor for various adsorption parameters, including the pH value of the solution, initial uranium concentration, bacteria concentration and the adsorption time and the adsorption process has been optimized. The adsorption kinetics and thermodynamics were investigated in detail and adsorption mechanism was proposed, providing another exploration for uranium pollution treatment with the adsorbent from ocean.

Experimental

Materials and reagents

The required concentration of uranium aqueous solution was prepared by dissolving a certain amount of $UO_2 (NO_3)_2 \cdot 6H_2O$ with distilled water. *Pseudomonas monteilii*. YL-1 was obtained from the South China Sea and incubated in a 250 mL Erlenmeyer flask containing 100 mL of liquid medium GPY (glucose 5 g/L, peptone 10 g/L, yeast extract 5 g/L, sea salt 10 g/L) at 30 °C on a rotary shaker for 24 h in anaerobic conditions. The mycelium was filtered, collected, dried, and then the bio-adsorption material was obtained.

1,2-cyclohexylenediaminetraaceticacid, 5-Sulfosalicylic acid dihydrate, trolamine, and 5-Br-PADAP and other reagents were purchased from Aladdin. Those reagents were of analytical reagent grade.

Adsorption experiments

A series of batch adsorption experiments were carried out in 250 mL Erlenmeyer flasks containing a certain amount of uranium solution, the initial pH of solution was adjusted by adding 0.1 mol/L HCl and NaOH solution. Then the *Pseudomonas monteilii* powders were added into uranium solution, and the flasks were transferred to the thermostat oscillator shaker for hours at 30 °C. After adsorption, 1.0 mL of sample was taken and centrifuged at 10,000 r/min for 10 min. And the uranium concentrations of samples were analyzed using UV-1750 UV/Vis spectrophotometer. All the experiments were carried out independently in triplicate to ensure the reproducibility of the method. The removal percentage (Y) and adsorption amount (Q) were calculated according to Eqs. (1) and (2):

$$Y = (C_0 - C_e)/C_0 \times 100\% \tag{1}$$

$$Q = (C_0 - C_e)/C_b \tag{2}$$

where Y is the removal efficiency, Q (mg/g) is the equilibrium bio-adsorption capacity, C_0 and C_e are the initial and equilibrium solution concentrations (mg/L), and C_b is the concentrations of *Pseudomonas monteilii* (g/L).

Detection of uranium

The uranium can react with 5-Br-PADAP to generate complex compound in the presence of NaF, 1,2-cyclohexylenediaminetraaceticacid, and 5-Sulfosalicylic acid at pH value around 7.5. The uranium concentrations of samples were detected by 5-Br-PADAP spectrophotometry using UV-1750 UV/Vis spectrophotometer at 578 nm. All the experiments were carried out independently in triplicate to ensure the reproducibility of the method.

Results and discussion

Effect of initial solution pH and ionic strength

The effect of initial solution pH and ionic strength on uranium adsorption was examined under the conditions of initial uranium concentration $C_0 = 50$ mg/L, *Pseudomonas monteilii* powders concentration $C_b = 0.3$ g/L, adsorption time $t = 60$ min. As shown in Fig. 1, the uranium adsorption capacity of *Pseudomonas monteilii*.YL-1 was strongly affected by the initial pH value and ionic strength. The sensitive effect of pH and ionic strength on adsorption indicates that the main mechanisms are attributed to ion exchange at low pH and surface complexation [19, 20]. The removal efficiency (Y) and adsorption capacity (Q) increase with the increase pH to a maximum value (pH 6.0) and then decrease with further increase of
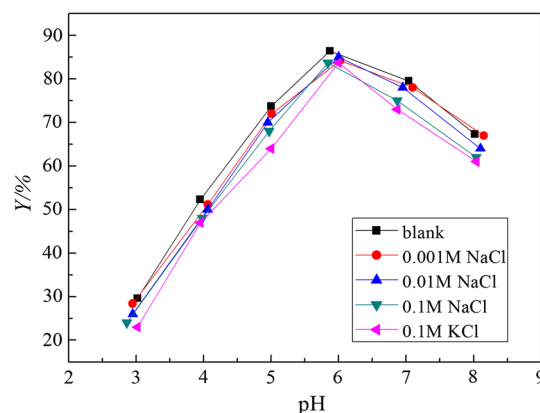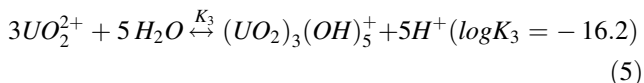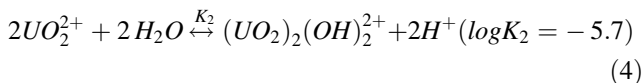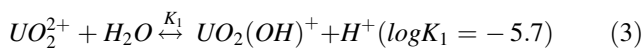

Fig. 1 Effect of initial solution pH and ionic strength on uranium adsorption

pH. The hydrolytic equilibrium equations of uranium in aqueous solution are shown by following Eqs. (3)–(5).

$$UO_2^{2+} + H_2O \overset{K_1}{\leftrightarrow} UO_2(OH)^+ + H^+ (logK_1 = -5.7) \quad (3)$$

$$2UO_2^{2+} + 2H_2O \overset{K_2}{\leftrightarrow} (UO_2)_2(OH)_2^{2+} + 2H^+ (logK_2 = -5.7) \quad (4)$$

$$3UO_2^{2+} + 5H_2O \overset{K_3}{\leftrightarrow} (UO_2)_3(OH)_5^+ + 5H^+ (logK_3 = -16.2) \quad (5)$$

At low pH, uranium exists in solution mainly in the form of UO_2^{2+}. Because of the smaller ion radius of H^+, the active adsorption sites of the *Pseudomonas monteilii*. YL-1 surface were occupied by H^+, reducing the number of binding sites for the combination of UO_2^{2+}, thus the uranium adsorption efficiency was very low [21]. When the pH was around 6.0, the UO_2^{2+} ions were easily attracted to the surface of the sorbent as the release of H^+. When pH value is over 6.0, hydrolysis species of uranium and the zero point of charge may result in the decline of adsorption removal efficiency and adsorption capacity of uranium [19, 22]. The slight decrease of uranium adsorption caused by the increasing ionic strength suggests that the adsorption of uranium is mainly via ion exchange with H^+ and Na^+ ions to saturate the exchange sites on the surface of *Pseudomonas monteilii* [23]. The recommended initial solution pH is 6.0 with the maximum adsorption removal efficiency and adsorption capacity of 86.4% and 144 mg/g, respectively.

Effect of initial uranium concentration

The initial uranium concentration provides an important driving force to overcome all mass-transfer resistance of uranium between the aqueous and solid phase [24]. The adsorption experiments were finished under the conditions of *Pseudomonas monteilii* powders concentration $C_b = 0.3$ g/L, adsorption time $t = 60$ min, pH = 6.0, and initial uranium concentrations increasing from 5 to 100 mg/L.

The effect of initial concentration of uranium on adsorption is shown in Fig. 2. The data reveal that the removal efficiency (Y) decreases with the increasing initial concentration of uranium, while adsorption capacity (Q) keeps increasing. The active adsorption sites of adsorbents are not fully occupied at low initial concentration of uranium, leading to the low adsorption uptake and high removal efficiency. With the increasing uranyl ions around the adsorption sites, more uranyl ions are captured by adsorbent and saturation of sorbents are obtained, resulting in the increase of adsorption capacity (Q) and the decrease of removal efficiency (Y) [25]. On the other hand,
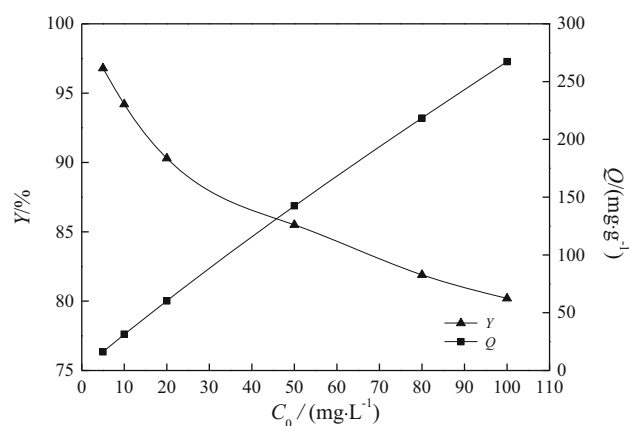

Fig. 2 Effect of initial concentration of uranium on adsorption of uranium

the formation of polymeric uranyl complexes at higher uranium concentration level leads to steric hindrance between the polymeric species, thus resulting in the decrease in removal efficiency. 100 mg/L is the recommended concentration of uranium due to the relatively high adsorption capacity (267.3 mg/g) and removal efficiency (80.2%).

Effect of adsorbent concentration

The experiments were carried out by varying the adsorbent concentration ranging from 0.1 to 0.6 g/L under the conditions of initial uranium concentration $C_0 = 100$ mg/L, pH = 6.0, adsorption time $t = 60$ min.

As shown in Fig. 3, the removal efficiency of uranium increases from 62.9 to 90.8% with the increasing adsorbent concentration. The adsorption sites on adsorbent increase due to the augment of adsorbent, leading to the increase of removal efficiency of uranium. Because of the adsorption resistance caused by ionic migration [26], the removal efficiency trends to be stable ($C_b > 0.3$ g/L). The
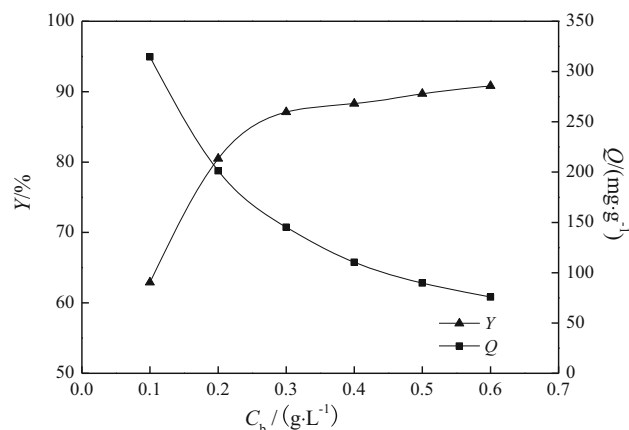

Fig. 3 Effect of adsorbent concentration on adsorption of uranium

adsorption capacity decreases from 314.5 to 75.7 mg/g with the increasing adsorbent concentration. The higher adsorbent concentration can produce a "screen" effect on the cell wall, protecting the binding sites, thus resulting in lower adsorption per unit of adsorbent [27].

Effect of adsorption time

The effect of adsorption time on the removal of uranium was examined under the conditions of initial uranium concentration $C_0 = 100$ mg/L, adsorbent concentration $C_b = 0.1$ g/L, pH = 6.0. As shown in Fig. 4, the removal efficiency of uranium and the adsorption capacity shows the same trend. Because of large amount of vacant adsorbent sites and high initial uranium concentration, the removal efficiency and the adsorption capacity of uranium increase significantly at the beginning of adsorption process. The adsorption efficiency remains unremarkable due to the gradual saturation of binding sites on the surface of adsorbent according to the establishment of adsorption–desorption equilibrium [28] 60 min latter. So the adsorption time of 60 min was chosen as the suitable adsorption time.

Adsorption kinetics

The kinetic of adsorption process mainly describes the potential for large-scale material transport and chemical reaction rate control steps. Kinetic model equations describe the quick kinetics of mass-transfer processes both between fluid phase and solid sorbent phase and in both phases [29]. Two kinetic models namely Lagergren's pseudo-first-order and pseudo-second-order kinetic models were applied to study the adsorption behaviors of *Pseudomonas monteilii* in this work, the equations are expressed as following [30]:
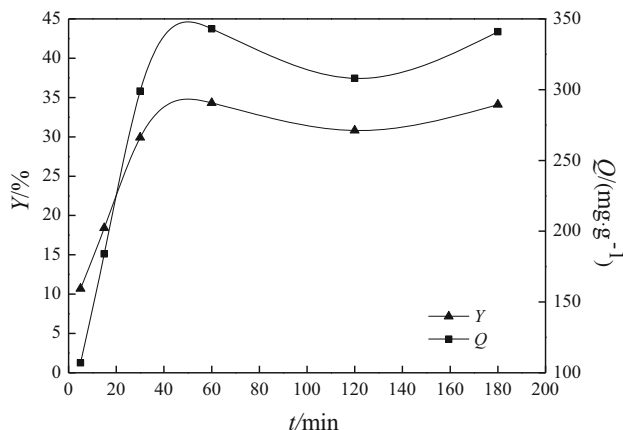
$$\frac{dq_t}{dt} = K_1(q_e - q_t) \, or \, \log(q_e - q_t) = -\frac{K_1 t}{2.303} + \log q_e \quad (6)$$

$$\frac{dq_t}{dt} = K_2(q_e - q_t)^2 \, or \, \frac{1}{q_t} = \frac{1}{K_2 q_e^2 t} + \frac{1}{q_e} \quad (7)$$

where q_t and q_e are the amount of the adsorbed uranium (mg/g) at time t (min) and at equilibrium, K_1 (min^{-1}) and K_2 (g/mg/min) are the adsorption rate constant of the pseudo-first-order Eq. (6) and pseudo-second-order Eq. (7).

In order to investigate the controlling mechanism of the adsorption process, The plots of $log(q_e - q_t)$ versus t and $1/q_t$ versus $1/t$ are shown in Figs. 5 and 6, and the calculated results are listed in Table 1. The experiments were carried out under the conditions of adsorbent concentration $C_b = 0.3$ g/L, initial uranium concentration $C_0 = 50$ mg/L, pH = 6.0.

As shown in Table 1, the correlation coefficients (R^2) for the pseudo-first-order is lower than that of Pseudo-second-order, indicating that pseudo-second-order kinetic model can adequately fit the adsorption data better for the *Pseudomonas monteilii* adsorbent. And the calculated value of q_e (144.93 mg/g) by the pseudo-second-order is also approximate to the experimental value (143.5 mg/g). So Pseudo-second-order model is more suitable to describe this adsorption process, implying that the adsorption of uranium is mainly controlled by chemisorption or strong surface complexation.

Adsorption isotherm

The interaction between adsorption capacity and bond energy, adsorbent and sorbate can be determined by isotherm models. The most commonly used equations are Langmuir and Freundlich isotherm models. The Langmuir model can be presented as:
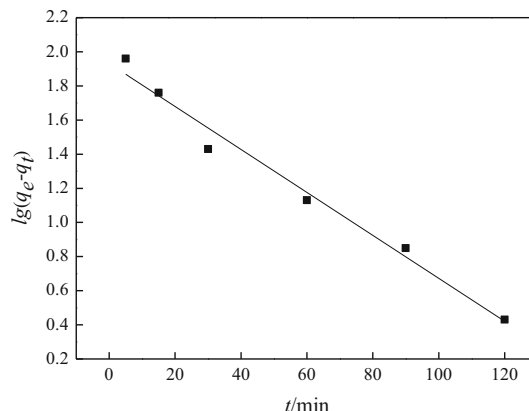

Fig. 4 Effect of adsorption time on adsorption of uranium

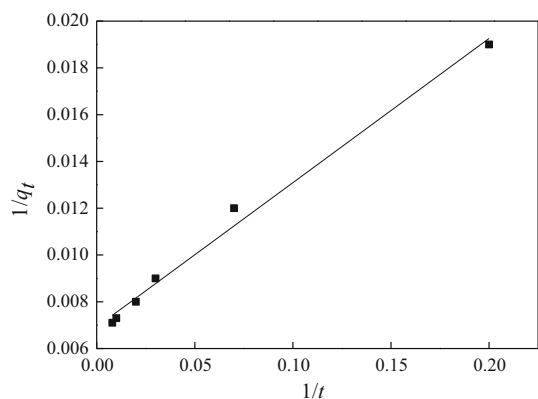**Fig. 5** The fitting curve for pseudo-first-order kinetic model

Fig. 6 The fitting curve for pseudo-second-order kinetic model

Table 1 The kinetic parameters of uranium adsorption

Pseudo-first-order			Pseudo-second-order		
K_1/pm	q_e/(mg·g^{-1})	R^2	$K_2 \times 10^{-3}$/pm	q_e/(mg·g^{-1})	R^2
0.0290	85.389	0.978	0.77	144.93	0.999

$$\frac{1}{q_e} = \frac{1}{bq_{max}C_e} + \frac{1}{q_{max}} \tag{8}$$

where C_e (mg/L) is the equilibrium concentration of uranium, q_e (mg/g) is the amount of uranium adsorbed on the adsorbent, q_{max} (mg/g) is the maximum adsorption amount and b is a constant related to adsorption. The Freundlich model is usually appropriate for heterogeneous adsorption and expressed as following:

$$\ln q_e = \ln K + \frac{\ln C_e}{n} \tag{9}$$

where K is the Freundlich constant related to the adsorption capacity and n is a constant which feature the system.

The Langmuir ($1/q_t$ versus $1/C_e$) and Freundlich ($\ln q_e$ versus $\ln C_e$) isotherms for the adsorption of uranium were plotted in Figs. 7 and 8, and a comparison of coefficients determined for the two adsorption isotherms were listed in Table 2. The Freundlich model fits the isotherm data with a higher correlation coefficient (R^2) of 0.997, better than the Langmuir model, indicating that the multilayer adsorption is the main adsorption process. In the Freundlich isotherm model, the performance of adsorption is described as "preferential adsorption" when $n > 1$ [31], and the calculated n is 1.6984, indicating that uranium can be easily adsorbed by *Pseudomonas monteilii* adsorbent.
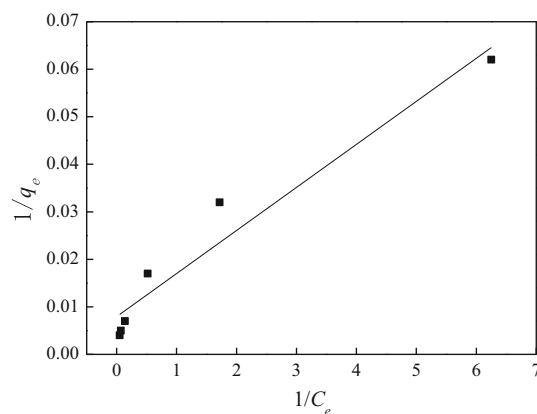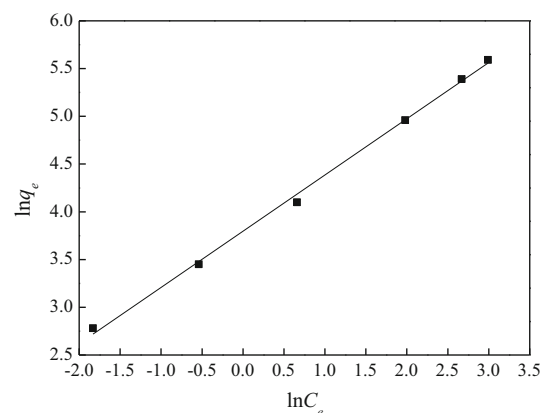

Fig. 7 Langmuir isotherm adsorption of uranium

Fig. 8 Freundlich isotherm adsorption of uranium

Thermodynamic study

Thermodynamic enthalpy (ΔH^0) and entropy (ΔS^0) are calculated by Van't Hoff Eq. (8). The values of ΔG^0 under different temperatures are calculated by Eq. (7).

$$\Delta G^0 = -RT \ln K \tag{10}$$

$$\ln K = \frac{-\Delta H^0}{RT} + \frac{\Delta S^0}{R} \tag{11}$$

$$K = \frac{C_0 \cdot v - C_e \cdot v}{C_e \cdot m} \tag{12}$$

Where K is the equilibrium constant, ΔH^0, ΔS^0, ΔG^0, and T are the enthalpy, entropy, Gibbs free energy, and temperature in Kelvin, respectively. R is the gas constant (8.314 J/mol/K).

Thermodynamic parameters of uranium adsorption are listed in Table 3. The negative values of ΔG^0 at various temperatures indicate the spontaneous nature of the adsorption process. The positive value of ΔH^0 indicates that the adsorption of uranium was endothermic. The positive value of ΔS^0 indicates that randomness increase at the solid-solution interface in the adsorption reaction and

Table 2 The isotherm parameters of uranium adsorption

Langmuir model			Freundlich model		
$b/(\mathrm{L \cdot mg^{-1}})$	$q_{max}/(\mathrm{mg \cdot g^{-1}})$	R^2	$K/(\mathrm{mg \cdot g^{-1}})/(\mathrm{mg \cdot L^{-1}})^{1/n}$	n	R^2
0.8786	125.63	0.934	44.542	1.6984	0.997

Table 3 The thermodynamic parameters of uranium adsorption

T/K	K	$\Delta G^0/(\mathrm{kJ \cdot mol^{-1}})$	$\Delta H^0/(\mathrm{kJ \cdot mol^{-1}})$	$\Delta S^0/(\mathrm{J \cdot mol^{-1} \cdot K^{-1}})$	R^2
303	13.485	− 6.554	4.765	37.360	0.999
313	14.390	− 6.939			
323	15.209	− 7.310			

that the influence of entropy was more remarkable than enthalpy of activation [32].

Adsorption mechanism

The scanning electron microscope (SEM) with energy dispersive spectroscopy (EDS) images for *Pseudomonas monteilii* before and after adsorption were shown in Fig. 9a and b, respectively. Compared with the EDS spectra of that in Fig. 9a, it is obviously that uranium is adsorbed on the *Pseudomonas monteilii* according to the appearance of EDS spectra peak of U in Fig. 9b. The transmission electron microscopy (TEM) images of *Pseudomonas monteilii* before and after adsorption were shown in Fig. 9c and d, respectively. The cell wall and inclusion of *Pseudomonas monteilii* were smooth and compact before the uranium adsorption. While the surface of the cell became rough due to the uranium bound to the functional groups after adsorption. Moreover, the inclusion of cell became incompact due to the enhanced permeability caused by the uranium adsorption on the cell wall.

The FTIR spectra were usually illustrated to identify the functional groups [33]. As shown in Fig. 10a, the broad and strong band around 3280 cm^{-1} should be attributed to
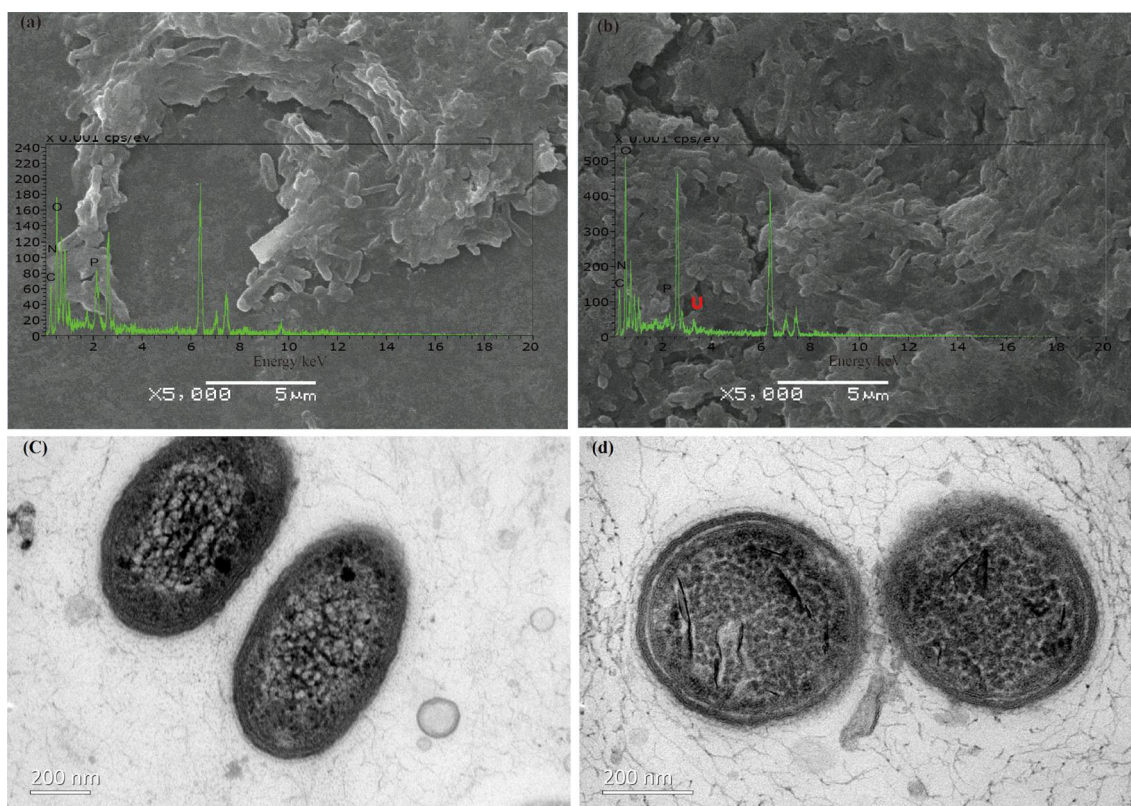

Fig. 9 The scanning electron microscope (SEM) with energy dispersive spectroscopy (EDS) images of *Pseudomonas monteilii* before (**a**) and after (**b**) adsorption. The transmission electron microscopy (TEM) images of *Pseudomonas monteilii* before (**c**) and after (**d**) adsorption
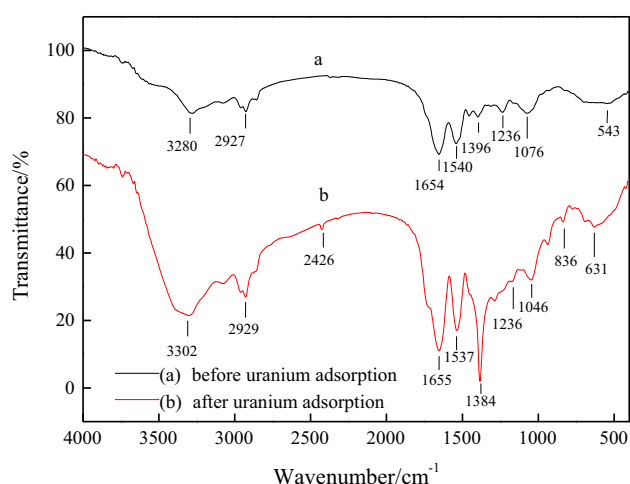
Fig. 10 FTIR spectra for *Pseudomonas monteilii* before and after adsorption of uranium

the stretching vibration of O–H and N–H groups, the peak at 2927 cm^{-1} are in accordance with symmetric or asymmetric C–H stretching vibration. The peak at 1654 cm^{-1} is due to –C=O stretching vibration and the peaks at 1540 and 1236 cm^{-1} are respectively assigned to N–H in-plane bending vibration of secondary amide and tertiary amide. The peak at 1076 cm^{-1} is due to the stretching vibration of C–O and C–N in *Pseudomonas monteilii* adsorbent. As shown in Fig. 10b, the FTIR spectrum of the adsorbent after uranium adsorption displays some changes. The adsorption of uranium is confirmed by the appearance of peak at 836 cm^{-1}, which is designated to the stretching vibration of UO_2^{2+}. Moreover, compared with the FTIR spectra of adsorbent before uranium adsorption, some peak sites are shifted from 3280 to 3302 cm^{-1}, 1654 to 1655 cm^{-1}, 1540 to 1537 cm^{-1}, 1076 to 1046 cm^{-1}, and the appearance of 2426 cm^{-1} is designated to the stretching vibration of N–H, indicating uranyl ions are bind to hydroxyl, amine, imino, and carbonyl groups on the modified sorbents surface by chemisorption or strong surface complexation.

Conclusions

The removal efficiency of 80.2% and adsorption capacity of 267.3 mg/g can be obtained under the conditions of pH of 6.0, initial uranium concentration of 100 mg/L, *Pseudomonas monteilii* powders concentration of 0.3 g/L, adsorption time of 60 min. Pseudo-second-order model is more suitable to describe this adsorption kinetic with a high correlation coefficients (R^2 = 0.999), and the Freundlich model fits the isotherm data well in adsorption process, implying that the adsorption of uranium is a multilayer adsorption process mainly controlled by chemisorption or

strong complexation. And thermodynamic study shows that the adsorption process is spontaneous and endothermic in nature. The SEM–EDS images reveal that uranium can be adsorbed to *Pseudomonas monteilii*. The surface and inclusion of *Pseudomonas monteilii* became rough and incompact after the adsorption. The result of FTIR spectra also shows that uranyl ions can be adsorbed on the surface due to the appearance of peak at 836 cm^{-1}, which is designated to the stretching vibration of UO_2^{2+}, and the functional groups on the surface of *Pseudomonas monteilii* interacting with uranium are mainly hydroxyl groups, carboxyl groups, amino groups and amide groups.

References

1. Wang G, Liu J, Wang X, Xie Z, Deng N (2009) Adsorption of uranium (VI) from aqueous solution onto cross-linked chitosan. J Hazard Mater 168(2–3):1053–1058
2. Chen S, Hong J, Yang H, Yang J (2013) Adsorption of uranium (VI) from aqueous solution using a novel graphene oxide-activated carbon felt composite. J Environ Radioact 126(4):253–258
3. Anirudhan TS, Bringle CD, Rijith S (2010) Removal of uranium(VI) from aqueous solutions and nuclear industry effluents using humic acid-immobilized zirconium-pillared clay. J Environ Radioact 101(3):267–276
4. Augustine S, Gagnaire B, Adam-Guillermin C, Kooijman SALM (2012) Effects of uranium on the metabolism of zebrafish, Danio rerio. Aquat Toxicol 118–119(2):9–26
5. Bampaiti A, Misaelides P, Noli F (2015) Uranium removal from aqueous solutions using a raw and HDTMA-modified phillipsite-bearing tuff. J Radioanal Nucl Chem 303(3):2233–2241
6. Semião AJC, Rossiter HMA, Schäfer AI (2010) Impact of organic matter and speciation on the behaviour of uranium in submerged ultrafiltration. J Membr Sci 348(1):174–180
7. Daher AM, Wanees SA, Kellah HMA, Ali AH (2014) Removal of uranium from sulfate leach liquor of salcrete deposits using tri-n-octyl amine. J Radioanal Nucl Chem 299(1):493–499
8. Gao MW, Zhu GR, Wang XH, Wang P, Gao CJ (2015) Preparation of short channels SBA-15-PVC membrane and its adsorption properties for removal of uranium(VI). J Radioanal Nucl Chem 304(2):675–682
9. Amirnia S, Ray MB, Margaritis A (2015) Heavy metals removal from aqueous solutions using Saccharomyces cerevisiae in a novel continuous bioreactor–biosorption system. Chem Eng J 264:863–872
10. Li S, Wang X, Huang Z, Du L, Tan Z, Fu Y, Wang X (2016) Sorption and desorption of uranium(VI) on GMZ bentonite: effect of pH, ionic strength, foreign ions and humic substances. J Radioanal Nucl Chem 308(3):877–886
11. Silva JIR, Ferreira ACDM, Costa ACAD (2009) Uranium biosorption under dynamic conditions: preliminary tests with Sargassum filipendula in real radioactive wastewater containing Ba, Cr, Fe, Mn, Pb, Ca and Mg. J Radioanal Nucl Chem 279(3):909–914

12. Jing B, Yao H, Fan F, Lin M, Zhang L, Ding H, Lei F, Wu X, Li X, Guo J (2010) Biosorption of uranium by chemically modified Rhodotorula glutinis. J Environ Radioact 51(6–7):382–387

13. Wang JS, Hu XJ, Wang J, Bao ZL, Xie SB, Yang JH (2010) The tolerance of *Rhizopus arrihizus* to U(VI) and biosorption behavior of U(VI) onto *R. arrihizus*. Biochem Eng J 51(2):19–23

14. Sar P, Kazy SK, D'Souza SF (2004) Radionuclide remediation using a bacterial biosorbent. Int Biodeterior Biodegrad 54(3):193–202

15. Kapoor A, Viraraghavan T, Cullimore DR (1999) Removal of heavy metals using the fungus *Aspergillus niger*. Biores Technol 70(1):95–104

16. Sangi MR, Shahmoradi A, Zolgharnein J, Azimi GH, Ghorbandoost M (2008) Removal and recovery of heavy metals from aqueous solution using *Ulmus carpinifolia* and *Fraxinus excelsior* tree leaves. J Hazard Mater 155(3):513–522

17. Sag Y, Kutsal T (2001) Recent trends in the biosorption of heavy metals: a review. Biotechnol Bioprocess Eng 6(6):376–385

18. Freitas OM, Martins RJ, Deleruematos CM, Boaventura RA (2008) Removal of Cd(II), Zn(II) and Pb(II) from aqueous solutions by brown marine macro algae: kinetic modelling. J Hazard Mater 153(1–2):493–501

19. Zhu W, Liu Z, Chen L, Dong Y (2011) Sorption of uranium(VI) on Na-attapulgite as a function of contact time, solid content, pH, ionic strength, temperature and humic acid. J Radioanal Nucl Chem 289(3):781–788

20. Gao Y, Shao Z, Xiao Z (2015) U(VI) sorption on illite: effect of pH, ionic strength, humic acid and temperature. J Radioanal Nucl Chem 303(1):1–10

21. Leyva-Ramos R, Bernal-Jacome LA, Acosta-Rodriguez I (2005) Adsorption of cadmium(II) from aqueous solution on natural and oxidized corncob. Sep Purif Technol 45(1):41–49

22. Bursali EA, Merdivan M, Yurdakoc M (2009) Preconcentration of uranium(VI) and thorium(IV) from aqueous solutions using low-cost abundantly available sorbent: sorption behaviour of uranium(VI) and thorium(IV) on low-cost abundantly available sorbent. J Radioanal Nucl Chem 283(2):471–476

23. Hu J, Shao D, Chen C, Sheng G, Li J, Wang X, Nagatsu M (2010) Plasma-induced grafting of cyclodextrin onto multiwall carbon nanotube/iron oxides for adsorbent application. J Phys Chem B 114(20):6779–6785

24. Khani MH, Keshtkar AR, Ghannadi M, Pahlavanzadeh H (2008) Equilibrium, kinetic and thermodynamic study of the biosorption of uranium onto Cystoseria indica algae. J Hazard Mater 150(3):612–618

25. Wang JS, Hu XJ, Liu YG, Xie SB, Bao ZL (2010) Biosorption of uranium (VI) by immobilized *Aspergillus fumigatus* beads. J Environ Radioact 101(6):504–508

26. Esposito A, Pagnanelli F, Lodi A, Solisio C, Vegliò F (2001) Biosorption of heavy metals by *Sphaerotilus natans*: an equilibrium study at different pH and biomass concentrations. Hydrometallurgy 60(2):129–141

27. Ozdemir G, Ceyhan N, Manav E (2005) Utilization of an exopolysaccharide produced by *Chryseomonas luteola* TEM05 in alginate beads for adsorption of cadmium and cobalt ions. Biores Technol 96(15):1677–1682

28. Hou D, Chen F, Yang SK, Yan XM, Long W, Zhang W, Jia XH, Tan N (2016) Study on uranium(VI) biosorption of marine-derived fungus treated by cetyltrimethyl ammonium bromide. J Radioanal Nucl Chem 307(2):1–8

29. Günay A, Arslankaya E, Tosun I (2007) Lead removal from aqueous solution by natural and pretreated clinoptilolite: adsorption equilibrium and kinetics. J Hazard Mater 146(1–2):362–371

30. Arica MY, Bayramoglu G, Yilmaz M, Bektaş S, Genç O (2004) Biosorption of Hg^{2+}, Cd^{2+}, and Zn^{2+} by Ca-alginate and immobilized wood-rotting fungus Funalia trogii. J Hazard Mater 109(1–3):191–199

31. Salem IA, El-Maazawi MS (2000) Kinetics and mechanism of color removal of methylene blue with hydrogen peroxide catalyzed by some supported alumina surfaces. Chemosphere 41(8):1173–1180

32. Anirudhan TS, Rijith S (2012) Synthesis and characterization of carboxyl terminated poly(methacrylic acid) grafted chitosan/bentonite composite and its application for the recovery of uranium(VI) from aqueous media. J Environ Radioact 106(2):8–19

33. Peng G, Ding D, Hu N, Yang Y, Wang X (2011) Adsorption characteristics of uranium by *Saccharomyces cerevisiae* by chemical modification. Ciesc Journal 62(11):3201–3206